The role of radial electric fields in the tokamaks TEXTOR-94, CASTOR, and T-10 *)

Guido Van Oost

Department of Applied Physics, Ghent University, Ghent, 9000 Belgium

James P. Gunn

Ass. EURATOM-CEA sur la Fusion Contrôlée, DRFC, CEA Cadarache, 13108 France

Alexander Melnikov

Nuclear Fusion Institute, RRC Kurchatov, Moscow, 123182 Russian Federation

Jan Stöckel

Institute of Plasma Physics, Ass. EURATOM/IPP.CR, Prague, 18221 Czech Republic

Michael Tendler

Alfvén Laboratory, RIT Stockholm, 10044 Sweden

Received 28 June 2001

Radial electric fields (E_r) and their role in the establishment of edge transport barriers and improved confinement have been studied in the tokamaks TEXTOR-94 and CASTOR, where E_r is externally applied to the plasma in a controlled way using a biased electrode, as well as in the tokamak T-10 where an edge transport barrier (H-mode) is obtained during electron-cyclotron resonance heating (ECRH) of the plasma.

The physics of radial currents was studied and the radial conductivity in the edge of TEXTOR-94 ($R = 1.75$ m, $a = 0.46$ m) was found to be dominated by recycling (ion-neutral collisions) at the last closed flux surface (LCFS) and by parallel viscosity inside the LCFS. From a performance point of view (edge engineering), such electrode biasing was shown to induce a particle transport barrier, a reduction of particle transport, and a concomitant increase in energy confinement. An H-mode-like behaviour can be induced both with positive and negative electric fields. Positive as well as negative electric fields were shown to strongly affect the exhaust of hydrogen, helium, and impurities, not only in the H-mode-like regime.

The impact of sheared radial electric fields on turbulent structures and flows at the plasma edge is investigated on the CASTOR tokamak ($R = 0.4$ m, $a = 0.085$ m). A non-intrusive biasing scheme that we call "separatrix biasing" is applied whereby the electrode is located in the scrape-off layer (SOL) with its tip just touching the LCFS. There is evidence of strongly sheared radial electric field and $\mathbf{E} \times \mathbf{B}$ flow, resulting in the formation of a transport barrier at the separatrix. Advanced probe diagnosis of the edge region has shown that the $\mathbf{E} \times \mathbf{B}$ shear rate that arises during separatrix biasing is larger than for standard edge plasma biasing. The plasma flows, especially the poloidal $\mathbf{E} \times \mathbf{B}$ drift velocity, are strongly modified in the sheared region, reaching Mach numbers as high as half the sound speed. The corresponding shear rates ($\approx 5 \times 10^6$ s^{-1}) derived from both

*) Presented at the 4th Europhysics Workshop "Role of Electric Fields in Plasma Confinement and Exhaust", Funchal, Madeira, Portugal, June 24–25, 2001

the flow and electric field profiles are in excellent agreement and are at least an order of magnitude higher than the growth rate of unstable turbulent modes as estimated from fluctuation measurements.

During ECRH in the tokamak T-10 ($R = 1.5$ m, $a = 0.3$ m), a regime of improved confinement is obtained with features resembling those in the H-mode in other tokamaks. Using a heavy ion beam probe, a narrow potential well is observed near the limiter together with the typical features of the L–H transition. The time evolution of the plasma profiles during L–H and H–L transitions is clearly correlated with that of the density profile and the formation of a transport barrier near the limiter. The edge electric field is initially positive after the onset of ECRH. It changes its sign during the L–H transition and grows till a steady condition is reached. Similar to the biasing experiments in TEXTOR-94 and CASTOR, the experimentally observed transport barrier is a barrier for particles.

1 Introduction

Since the H-mode was discovered in ASDEX [1], many theories have pointed to the possible decisive role of E_r in the creation of transport barriers (i.e. zones of finite radial extent where particle and/or heat diffusivity are depressed) and in the L–H bifurcation mechanism. The H-mode can also be triggered by externally inducing an E_r in the plasma (independently of other plasma parameters) as demonstrated in the tokamaks CCT [2] and TEXTOR-94 [3] and later in many other machines (see review [4]). By inserting a biased electrode in the plasma edge, an edge radial electric field and its shear can be externally induced and controlled. High space and time resolution edge diagnostics enable to investigate the dynamics of E_r and its effects. These electrode biasing experiments have contributed significantly to the understanding of the H-mode phenomenon and of the effects of E_r on plasma transport.

In more detail, the electric field profile in a tokamak is governed by the subtle balance between parallel dynamics (neoclassical viscosity) and the anomalous transport of the angular momentum. The impact of the magnetic field geometry (due to the presence of a separatrix or the appearance of chains of magnetic islands etc.) is provided by poloidal variations of parallel and perpendicular flows emerging due to changes of the fine structure of the magnetic field in a tokamak. The focus is on the interface between the helical type of the chain of magnetic islands located on rational surfaces and the rest of the bulk of the plasma core in a tokamak. X-points of the chain of islands are stringently defined as well as O-points. The bottom line is that there is the poloidal variation of the electric field due to poloidal variations in proximity of adjacent magnetic surfaces in the vicinity of the chain of islands. Thus, the poloidal velocity shear is locally significantly amplified thereby triggering the front of improved confinement.

The present paper deals with the study of radial electric fields (E_r) and their role in the establishment of edge transport barriers and improved confinement in the circular limiter tokamaks TEXTOR-94 in Jülich and CASTOR in Prague where E_r is externally applied to the plasma in a controlled way using a biased electrode, as

well as in the tokamak T-10 in Moscow where a (spontaneous) edge transport barrier (H-mode) is obtained during electron-cyclotron resonance heating (ECRH) of the plasma. The (spontaneous) H-mode has been obtained in a variety of tokamaks mainly with elongated plasma cross section and divertor, and recently also in the limiter tokamak T-10 with ECRH as the only auxiliary heating. An (induced) H-mode can also be triggered externally by imposing an electric field and the resulting $\mathbf{E} \times \mathbf{B}$ rotation in tokamaks like TEXTOR-94 and CASTOR.

2 Electrode biasing on TEXTOR-94

The main aims of these pioneering studies, which started in the early nineties were:

- to contribute to the understanding of the establishment of improved confinement (such as the H-mode) and of the effects of radial electric fields on particle confinement.
- to study the impact of $\mathbf{E} \times \mathbf{B}$ velocity shear on the reduction of turbulence.
- to study the effects of radial electric fields on particle flows in the plasma boundary which strongly affect plasma exhaust.

2.1 Experimental set-up

The set-up of the edge polarisation experiment is shown in Fig. 1. The electrode has a mushroom-shaped head that is inserted about 5 cm beyond the toroidal belt limiter (ALT-II). The voltage is applied between the electrode and the limiter, which is grounded to the potential of the first plasma-facing wall (named as liner). An insulating boron-nitride sleeve assures that the bias potential is only imposed on flux surfaces intersecting the electrode head. More details on electrode biasing in TEXTOR-94 can be found in [3, 5].

Usually the bias voltage V_{E} in the experiments reported here was slowly varied over time from 0 up to maximum 600 V. The plasma parameters are $B_{\mathrm{t}} =$

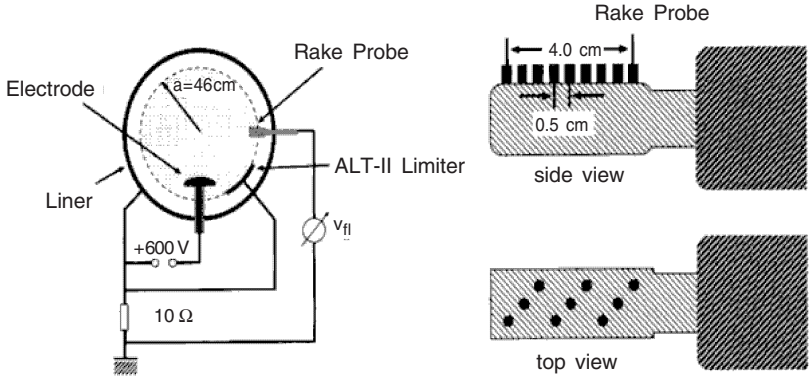

Fig. 1. Schematic drawing of the polarisation set-up and of the rake probe.

2.33 T, $I_p = 210$ kA and the pre-bias central line-averaged electron density $n_e = 1 \times 10^{19}$ m^{-3}. The spatial location and the magnitude of the electric field are imposed by the magnitude of the radial current and by the profile of the radial conductivity, determined by parallel viscosity and ion-neutral collisions [6].

The radial electric fields are determined using a Langmuir probe (rake probe) consisting of a boron-nitride head carrying nine carbon (CFC) tips (length 4 mm, radius 1.6 mm), radially distributed over 4 cm, and measuring the profile of the floating potential V_{fl} with a radial resolution of 5 mm. The tips are aligned perpendicularly to the magnetic field such that probe shadowing is avoided. The probe is at a fixed position during the whole discharge. The radial electric field is then found as

$$E_r = -\nabla V_{pp} \approx -\nabla V_{fl} - 3\frac{k\nabla T_e}{e},$$

where V_{pp} is the plasma potential. Since in these experiments ∇V_{fl} is of order 100 V/cm, we neglect the contribution from the temperature gradient, which is typically less than 10 eV/cm and remains small in the high confinement regime (similar approach for determination of E_r in CASTOR, see Section 3). The time resolution of the rake probe is 40 μs.

Mach probes were tested and optimised to determine parallel and perpendicular particle flows in the plasma edge and SOL [7], allowing together with the well diagnosed pumped toroidal belt limiter ALT-II the study of particle exhaust.

The electron density profiles are obtained by means of a Li–beam spectroscopy diagnostic as described in [8]. As a key issue in this investigation is the detailed spatial and temporal correlation of the field and density changes, it is important to note that the atomic beam and the rake probe are mounted at the same equatorial outboard port, toroidally separated only by 12 cm, which minimises errors in determining their relative radial allocation. The relatively poor time resolution of the Li-beam (typically 10 ms, occasionally 5 ms) is made up for by the capability of varying the rate of increase of the applied voltage at will (2 s ramps are typical), thus allowing a tuning of the physical time scales to that of the diagnostic.

Changes in the global particle confinement time τ_p are inferred from the ratio of the total number of electrons in the discharge N_e^{tot} to the total ionisation rate at the plasma periphery (i.e. the hydrogen source term). The latter requires a detailed bookkeeping of recycling at the limiter, the wall and the electrode. For this purpose we use a tangentially viewing H_α-camera covering about one third of the torus and providing a global image with localisable contribution from each source. The total recycling due to each source can be evaluated by multiplying the emission, measured in judiciously selected boxes that are representative for that source in the global image, with a correction factor inferred from the viewing geometry [9]. The ALT-II limiter and the wall present a toroidally symmetric edge recycling, the electrode does not. The latter's contribution is therefore carefully analysed by supplementing its partial observation on the global image by an independent electrode specific viewing system.

2.2 Physics of orthogonal conductivity

H-mode behaviour is usually linked to the existence of radial electric fields or to their radial gradient at the edge of tokamaks. The mechanisms were investigated by which such fields are induced in the plasma edge and by which the profile shaping is obtained when radial currents are imposed by electrode polarisation. Detailed experimental field measurements were successfully compared with a theoretical conductivity model in which neoclassical non-ambipolar transport and mobility through ion-neutral collisions are predominant [6]. Strong neoclassical viscosity in the bulk plasma allows significant fields to develop only at the very edge of the plasma. There a delicate balance between viscosity and ion-neutral friction takes place, which strongly affects the magnitude and spatial location of the fields as well as the threshold condition for L–H field bifurcation.

Several effects are neglected in the present analysis: for example, the convective derivative, toroidal rotation, fluctuations, perpendicular viscosity and the role of impurities in the radial transport. It is, nevertheless quite surprising how the different theories on viscous damping are capable of achieving better than just 'order of magnitude' agreement in the radial conductivity. The degree of agreement obtained might indicate that our modelling has indeed identified the main contributors to the physics of radial current flow. At the very edge of the tokamak, mobility due to ion-neutral collisions appears to be very important; deeper in the plasma the current transport is practically exclusively due to non-ambipolar neoclassical transport. The reason why these two suffice might very well be that other transport mechanisms are intrinsically ambipolar, contributing to the electron and ion outflows, but not to a radial current. Electrostatic turbulence, for example, is considered to be the most important mechanism for particle outflow, and yet it is not expected to drive a considerable radial current [10]. Electrostatic turbulence can thus, on the one hand, easily dwarf the neoclassical ambipolar particle flux in a plasma without imposed radial fields. As the turbulence, on the other hand does not sustain a considerable current, the neoclassical feature shows up in experiments where current is forced through the edge and the neoclassical transport coefficients are effectively experimentally checked at radii smaller than 44 cm ($a = 46$ cm).

This study also contributed to the understanding of "spontaneous" H modes.

1. The electric field shape in the biasing experiments appears to be imposed by the conductivity profile. In the spontaneous H mode case, an additional shaping factor might appear. To the extent that the rotation driving force might be provided by the ion loss current [11], the poloidal Larmor radius provides extra shaping.

2. Many explanations for the L–H bifurcation are based on poloidal rotation and differ in the mechanism for rotating the edge plasma: for example, ion orbit losses [11], Stringer spin-up [12] and Reynolds stress [13]. In all cases the driving force should be balanced by damping.

   It can be concluded that in all these schemes both ion-neutral and neoclassical damping will be active. On the one hand, the neoclassical feature of

reduced damping at high speed can in all cases lead to bifurcation. The pronounced effect of ion-neutral collisions, on the other hand, on the H mode phenomenon can be inferred from the experimental observations on the role of recycling: increased recycling by excessive gas puffing or by proximity of limiters quenches the H-mode or affects the power threshold.

3. This study appears to give a rather limited predictive credit to scaling laws for the H mode power threshold [14], as the edge values of the electron and ion densities and of the temperature and the neutral density probably depend in a rather intricate way on the global plasma parameters as well as on the wall conditioning.

2.3 Impact of edge electric fields on bulk confinement and exhaust

Particle confinement (τ_p) of deuterium and of impurity ions as well as energy confinement (τ_E) were investigated [3]. For positive fields, which remain below the threshold for the L–H transition, an interesting regime of reduced particle confinement without noticeable energy confinement loss was found. A strong asymmetry in the edge density profiles with respect to the electric field sign is observed at low voltages. Above the threshold, H-mode behaviour with improved energy confinement and especially particle confinement can be produced with either polarity of the applied electric field. It was, however found that whereas the energy confinement in positive H-modes (H_+) is at least as good as that in negative ones (H_-), the ratio $\tau_\mathrm{p}/\tau_\mathrm{E}$ is about three times lower in the former case.

The changes in the edge profiles of important parameters, as a function of the imposed electrode potential were investigated. Of particular interest is the electric field profile. The scale length of E_r is in principle imposed by the scale lengths of the current density j_r and the radial conductivity σ_r or a combination of both. Since j_r in our experiments is essentially constant over the outer 5 cm of the plasma, only σ_r is capable of tailoring E_r. In other experiments, where j_r is mainly constituted by the ion losses, an additional constraint is introduced. The TEXTOR-94 experiments showed, however, that even under the latter conditions the role of σ_r should not be neglected.

The electron density profile clearly steepens in the plasma edge, but no equivalent feature is seen in the temperature profile, implying the formation of a particle transport barrier only (similar observation in CASTOR). The increased confinement in the H-mode could be linked to an electron thermal conductivity χ_e^c, which scales as $1/n_\mathrm{e}$ and a density rise resulting from the particle barrier.

Particle confinement was thus a central issue in this investigation. It was studied by injecting trace elements (Ne, He) into the plasma and observing their exhaust rates. Since the decay time of the concentration of these elements is quite exponential, an effective confinement time τ_p^* can be defined. The confinement of the main ion component deuterium was derived by balancing the loss rate with the ionisation rate, inferred from D_α measurements as described in [3]. Since τ_p^* constitutes the main descriptor, more study is definitely needed to completely characterize τ_p

under all conditions. For example, the fact that τ_p^* has no strong species (Ne, He, D_2) dependence does not mean that this is also automatically true for τ_p. Other conclusions, however appear to be more definite. For positive fields at levels below the threshold or the L–H transition an interesting regime was shown to exist. This regime has reduced particle confinement and no noticeable energy confinement loss. Since the edge measurements yield similar profiles and energies for the exhausted particles in the H_+ and H_- modes, τ_p is also very likely to follow τ_p^* under these circumstances.

The particle confinement is typically increased by a factor of about two in H_+ and by a factor of more than four in H_-. Also the energy confinement is increased with either polarity of the applied electric fields. However, the energy confinement in positive H-modes is at least as good as that in negative H-modes [3].

Combining the energy and particle confinement results, one can conclude that the ratio of τ_p/τ_E is about three times lower in the H_+ mode than in the H_- mode. However, conditions with particle confinement times much higher than the energy confinement time are not desirable in a reactor. In Ref. [15] it was argued that the ratio τ_{He}^*/τ_E should remain below ten to allow ignited, stationary D-T operation. The present results yield values in excess of what would be tolerable: about 20 in beam heated L-mode discharges, i.e. inside the range between 10 and 30 found in an earlier investigation on TEXTOR-94 [16], about 40 in the H_+ conditions and at least 100 in the H_- modes (extrapolating the D_2 and Ne results). The above figures may very well be machine dependent and could be improved by providing a better exhaust efficiency. Given the differences between the H_+ and the H_- conditions, however, it would appear to be of considerable interest to find schemes, other than electrode biasing, to achieve the preferential electron loss from the plasma that is necessary for setting up positive H-modes (see e.g. separatrix biasing on CASTOR in Section 3).

Mach probes were tested and optimised on TEXTOR-94 to determine parallel and perpendicular particle flows in the plasma edge and SOL [7], allowing together with the well diagnosed pumped toroidal belt limiter ALT-II the study of particle exhaust. See also the discussion on flow measurements on CASTOR in Section 3.

3 Separatrix biasing on CASTOR

The impact of sheared electric fields on the structure of edge fluctuations and plasma flows is investigated on the CASTOR tokamak. A non-intrusive biasing scheme is applied, whereby the electrode is located in the SOL, but its top is just touching the separatrix.

It has been demonstrated on many machines with a variety of discharge- and heating conditions as well as edge biasing schemes that $\mathbf{E} \times \mathbf{B}$ flow velocity shear is a robust and universal mechanism to reduce plasma turbulence and to establish transport barriers. The CASTOR edge biasing arrangement and novel diagnostics have recently contributed to the improved understanding of the physical mecha-

nisms involved. On CASTOR, the biased electrode can be located at two different positions with respect to the separatrix:

– "Standard" configuration of biasing experiments: The electrode is located deep in the edge plasma, i.e. in the region with closed magnetic field lines, like in the case of TEXTOR-94. Consequently, the radial gradient of the radial electric field is amplified between the electrode and the separatrix. All results presented pertain to positive biasing. Although this arrangement has contributed significantly on different machines to reveal the key role of electric fields, see e.g. [17–19], it can hardly be accepted in practice in large-scale experiments with high thermal loads.
– Biasing of separatrix: Alternatively, the biased electrode is inserted just into the scrape-off layer (SOL) [20]. In this case, the thermal load should certainly be smaller than in the previous case and such scheme can be employed as non-intrusive one. It was suggested [21] that separatrix biasing (i.e. imposing a boundary condition on the separatrix) is an efficient way to create strongly sheared electric fields, thereby affecting plasma flows and turbulent structures.

3.1 Set-up of biasing experiments

The main parameters during electrode biasing experiments on the tokamak CASTOR ($R = 0.4$ m, $a = 0.085$ m) are $B_t = 1$ T, $I_p = 9$ kA (i.e. high q operation) and line averaged densities $n_e \approx 1 \times 10^{19}$ m^{-3}. A mushroom-like biasing electrode (made of carbon) is inserted into the plasma from the top of the torus and biased with respect to the vacuum vessel by a pulsed voltage.

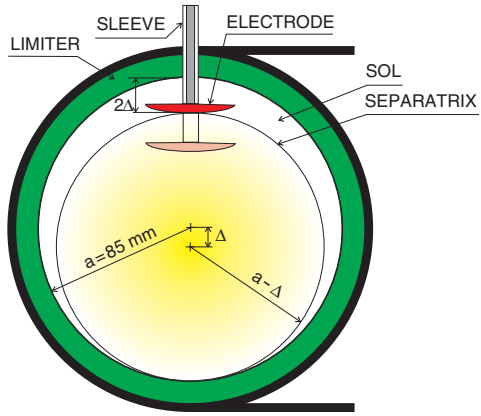

Fig. 2. Poloidal cross section of the CASTOR tokamak schematically showing the location of plasma column and biasing electrode at the "standard" and at the "separatrix biasing" arrangements, respectively. As seen from the figure, the mushroom electrode is hidden in the SOL and its top is just touching the separatrix in the last case.

It has been found on the CASTOR tokamak that separatrix biasing is effective only if the SOL is broader than the radial extent of the biasing electrode. For this purpose, the plasma column is shifted downwards, as schematically shown in Fig. 2.

Therefore, the minor radius of the plasma column is not determined by the radius of the poloidal limiter, but is reduced to $a - \Delta$. As a consequence, the SOL becomes broader (width 2Δ) at the top of the torus. The connection length in this region is long compared to the circumference of the torus ($2\pi R$). The location of the separatrix (the last closed flux surface) is not determined by magnetic diagnostics on CASTOR, but is taken as the position of the velocity shear layer (VSL), where the radial electric field and the poloidal flow velocities are measured to be zero. The VSL position is deduced from the floating potential profile, measured by the rake probe in every shot. The radial position of the separatrix can vary within several mm, depending on the discharge conditions.

Because of the strong poloidal asymmetry of the scrape-off layer (SOL), the main diagnostics of the biasing experiment are located at the same poloidal angle as the electrode, i.e. at the top of the torus.

3.2 Probe diagnostics

The edge plasma is diagnosed on CASTOR by electrical probes. Some of them (such as the rake probe and the poloidal probe array) were already described earlier [22]. Here, we present two novel diagnostics to investigate plasma flows and properties of turbulent structures in the radial and poloidal direction.

Flow measurements

The flow measurements in CASTOR using the Gundestrup and Rotating Mach probe are discussed in Refs. [7,23–26,34].

2D matrix of Langmuir probes

The probe array consists of 64 tips arranged into 8 rows and 8 columns [20]. The distance between the rows, $d_\mathrm{r} = 4.5$ mm, defines the radial resolution. The distance between the columns is $d_\mathrm{p} = 6$ mm. The carbon tips (diameter 2 mm) are fixed in an insulating plate made of boron nitride. The individual tips measure either the floating potential or the ion saturation current. The mode of operation can be switched between shots. The data are digitized at a rate of 1 μs/sample. The probe head itself is made of stainless steel, but covered by a layer of boron carbide (B_4C) to improve its compatibility with the plasma and to reduce its conductivity. The probe head is mounted on a manipulator allowing its radial motion on a shot-to-shot basis.

The position of the probe head in a poloidal plane of the CASTOR tokamak is shown schematically, but in scale, in Fig. 3. It is immersed into the edge plasma so that the magnetic field lines are perpendicular to the probe matrix, being located at the top of the torus (135° toroidally away from the ion side of the main poloidal limiter).

In the same figure, a snapshot of the distribution of the floating potential in the poloidal plane is shown as well. The dark regions in the plot denote the floating

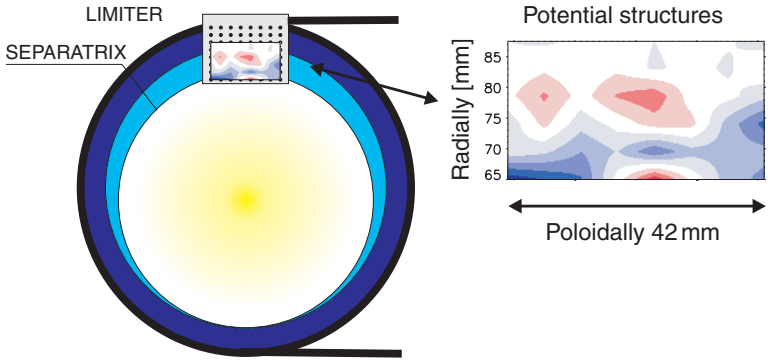

Fig. 3. Position of the 2D matrix of Langmuir probes in the poloidal plane of the CASTOR tokamak (in scale) together with a snap shot of potential structures. Only six rows of tips were active in this discharge.

potential lower than a mean value (potential valleys), while the bright patterns correspond to the potential hills. Even a visual inspection of such a map indicates that turbulent structures are smaller then the dimension of the array but larger then the distance between the tips. Pioneering research with a similar array was performed on the CALTECH tokamak [27].

The area of the probe head represents a non-negligible part of the poloidal cross section. However, the radial profiles of the floating potential, measured for several radial positions of the probe head showed that the shadowing due to the array does not dominate the edge plasma.

3.3 Experimental results

Evolution of polarised discharges

The evolution of the global plasma parameters with both biasing schemes is compared in Fig. 4 for similar discharge conditions.

The electrode is positively biased ($U_\mathrm{b} = +200$ V). As seen in the figure, a current of about (35–40) A is drawn by the electrode during the biasing period. The line averaged density increases substantially with biasing in both cases. However, the evolution of the H_α spectral line intensity H_α exhibits different shapes. For the "standard" configuration, the intensity drops immediately with biasing, which evidently implies a reduction of recycling and results in improvement of the global particle confinement (by 80%). On the contrary, at separatrix biasing, the H_α emission slightly increases during the initial phase of the biasing period. Nevertheless, the global particle confinement time increases substantially (by $\approx$ 50%), as seen in the bottom panel of Fig. 4.

A substantial difference between the radial profile of the floating potential, U_FL, for both biasing schemes is apparent from Fig. 5.

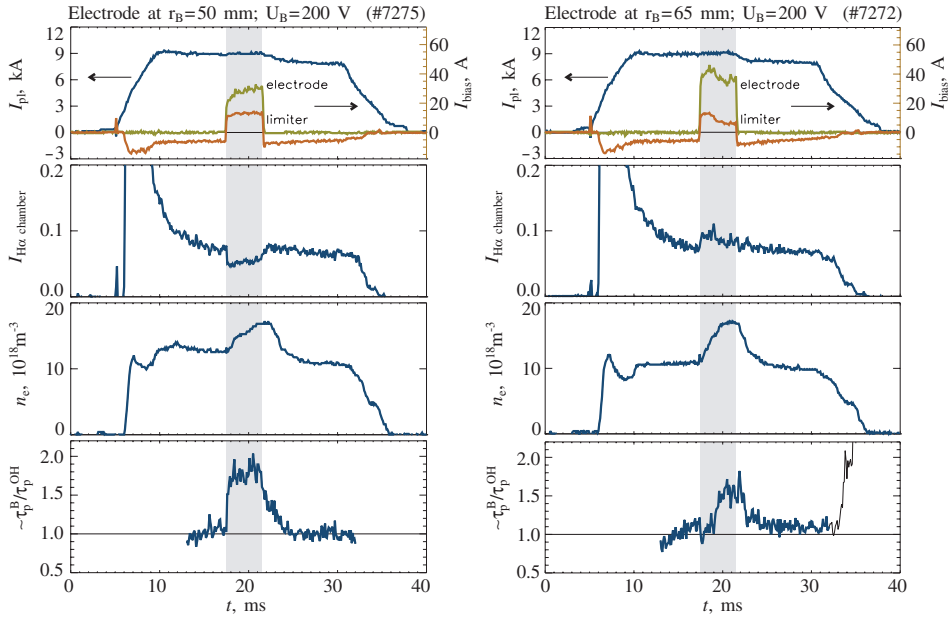

Fig. 4. Evolution of polarised discharges at "standard" (left) and "separatrix biasing" (right). From top to bottom: electrode current and return current to the poloidal limiter together with the evolution of the plasma current; intensity of the H_α spectral line; line averaged density; relative improvement of the global particle confinement time.

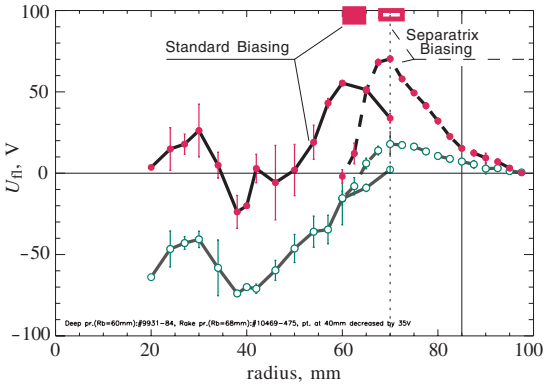

Fig. 5. Comparison of the radial profile of the floating potential without (grey curves) and with biasing (black curves), plotted for two positions of the biasing electrode (U_b = +100 V): r_{bias} = 60 mm — "standard" biasing scheme (solid lines), measured by a single floating probe on a shot-to shot basis; r_{bias} = 68 mm — "separatrix" biasing (dashed lines), measured by a rake probe.

At "standard" biasing, the potential of the whole plasma column is shifted by $\approx U_b$ and, consequently, the radial electric field E_r is amplified between the electrode and the separatrix. On the other hand, at separatrix biasing, the potential is affected only in a relatively narrow region near the separatrix and the radial electric field is amplified at both sides of the electrode. Consequently, the radial electric field is highly sheared in that region and affects significantly the plasma flows and the turbulent structures. The strongest shear appears at the innermost side. The flow and fluctuation measurements described below have been performed with separatrix biasing.

Flow and fluctuation measurements in sheared electric fields

Figure 6 shows radial profiles measured during separatrix biasing, ($U_b = +150$ V, the electrode position at $r = 70$ mm). The top panels show the potential/electric

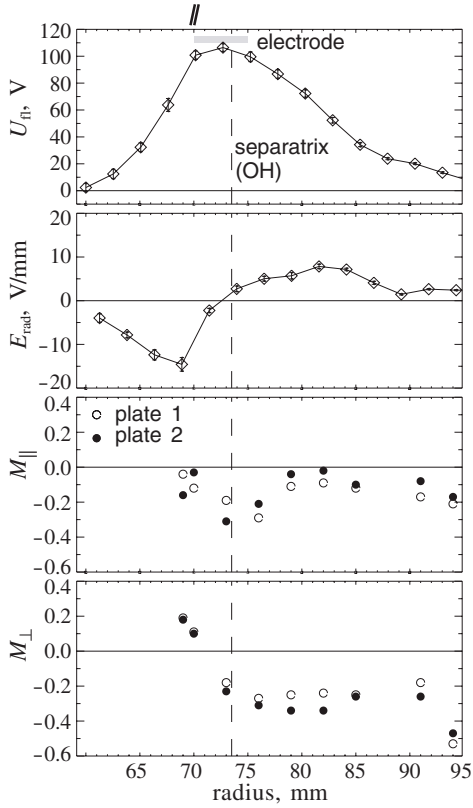

Fig. 6. Radial profiles at separatrix biasing ($U_b = +150$ V). Top panels: floating potential and radial electric field. Bottom panels: parallel and perpendicular Mach numbers deduced from both plates (plate 1 — circles, plate 2 — bullets). The dashed vertical line denotes the position of the separatrix in the non-polarised discharges.

field profiles measured by the rake probe. The bottom panels show the parallel and perpendicular Mach numbers, measured by the rotating Mach Probe [25].

It is evident from the figure that the layers of the largest perpendicular flow velocity shear and the sheared region of the radial electric field appear to coincide ($r = (69–72)$ mm). Moreover, the values of the $\mathbf{E} \times \mathbf{B}$ shear rate, deduced from the radial electric field profile and the shear of the flow velocity v_{pol} derived from the $M_\perp$ profiles are comparable in this region $\Delta v_{\mathrm{E\times B}}/\Delta r \approx \Delta v_{\mathrm{pol}}/\Delta r \approx 5 \times 10^6$ s^{-1} and significantly exceed the typical growth rate of unstable modes. This growth rate is estimated from fluctuation measurements as the reciprocal value of the autocorrelation time, $\gamma = 1/\tau_{\mathrm{A}} \approx (5–20)\times 10^4$ s^{-1} [22].

To demonstrate the strong impact of sheared flows on the edge turbulence, the data measured by the poloidal probe array was used [28]. The spatial-temporal correlation functions are calculated and the result is shown in Fig. 7, which consists of 18 panels. Each row of the figure corresponds to a single radial position of the probe array, indicated in the right-hand side column of the figure. The left panel of a row characterises the turbulence in the OH phase of the discharge, the right one corresponds to the polarised phase ($U_{\mathrm{b}} = +200$ V).

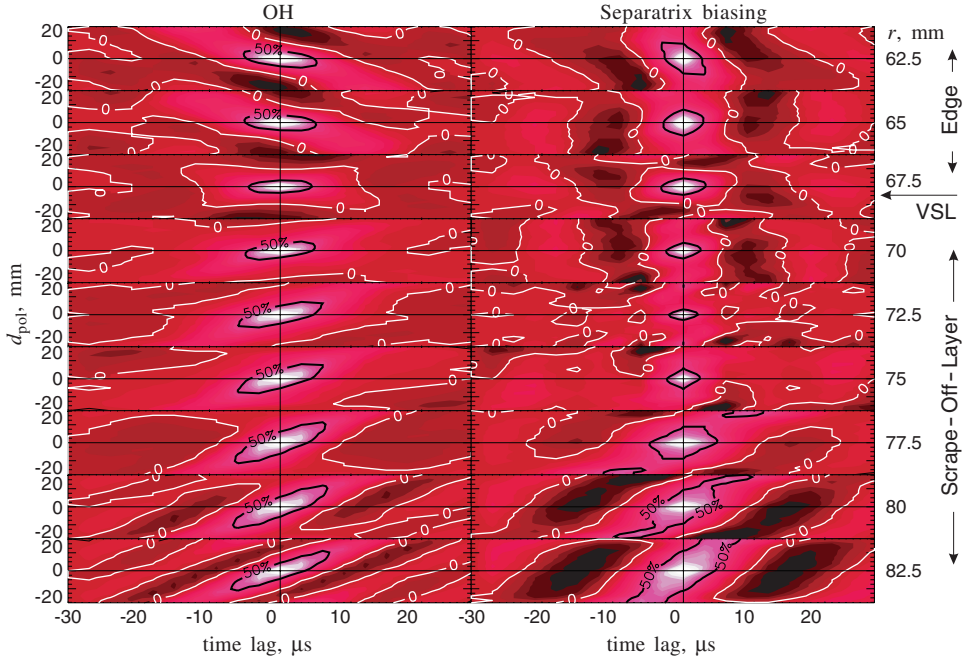

Fig. 7. Spatial-temporal correlation functions in the poloidal direction for several radial positions of the poloidal probe array. Position of the separatrix $r_{\mathrm{s}} = 67$ mm.

Each panel shows the spatial–temporal correlation function. The bright patterns of elliptical shape are the regions of the highest correlation ($> 50\%$). Their

dimension in the y-direction corresponds roughly to the poloidal extent of the turbulent structures, while the x-dimension corresponds roughly to their life time. The poloidal propagation velocity of the structures is deduced from the slope of the correlation patterns. A more precise interpretation of such 2D correlation is given in [29].

The position of the separatrix is seen in the left column at $r = 67$ mm, where the reversal of poloidal propagation is well apparent. The biasing electrode is located approximately at the same radius. Thus, the region with the highest shear flow is formed there during biasing. A strong de-correlation of the turbulent structures in the poloidal direction as well as in time is evident from a dramatic reduction of the size of the correlation patterns in this range of radii. A similar effect is observed also in the radial direction [30], using the data from the rake probe. The simultaneous poloidal/radial correlation analysis at separatrix biasing (using data from the 2D matrix) is in progress.

4 H-mode in T-10 with ECRH

During electron cyclotron resonance heating (ECRH) in the T-10 tokamak ($R =$ 1.5 m, $a = 0.3$ m), a regime of improved confinement was obtained with features resembling those observed in the enhanced confinement regime with an external transport barrier (H-mode) [31]. The Heavy Ion Beam Probe (HIBP) diagnostic was used to directly measure the local values of the plasma potential in the core and edge plasmas [32].

4.1 Experimental conditions

This regime has been investigated over a wide range of toroidal magnetic fields from $B_\mathrm{t} = 2.42$ T (on-axis microwave power deposition) to $B_\mathrm{t} = 2.14$ T (off-axis heating). The microwave power absorbed in the plasma attained 0.8 MW. Note that the microwaves (second ECR harmonic, X-mode) were launched into the plasma at an angle of 21° to the direction of the major radius R with a view to EC current drive. However, at plasma currents I_p above 180 kA, the driven current comprises only a small fraction of I_p, so that its influence on the processes studied here was negligible. To clarify the main features of the H-mode, the plasma density and the safety factor q were varied (plasma current varied between 180 and 330 kA at $B_\mathrm{t} = 2.42$ T). The limiter was located at 30 cm.

The HIPB is the only diagnostic capable of directly measuring the plasma potential in the core and edge plasmas. A Tl^+ ion beam with energy up to 250 keV and intensity of a few dozen μA was used to probe the outer half of the plasma column at the low field side ($r =$(18–30) cm for 2.5 T, and $r =$(7–30) cm for 1.5 T). The local value of the plasma potential can be measured by the change of the beam energy in the sample volume. The intensity of the secondary beam indicates the local density. The specific feature of this system is the presence of toroidal electrostatic steering plates in the diagnostic port in front of the entrance of the energy analyzer. These plates correct the toroidal displacement of the secondary ions with

a voltage pulse of up to 5 kV. The power supply provides measurements during 7 ms of the correcting pulse flat top every 20ms. The analyzer was inclined toroidally in accordance with the 3D trajectory calculation in order to reduce the amplitude of the correcting voltage, and to avoid that arcs affect the secondary beam signal. These modifications allow measurements in OH and ECRH plasmas within almost the whole operational range.

The HIBP was used in two main operating regimes:

- *Shot by shot measurements* allow to obtain the time evolution of the plasma parameters in every point of the detector grid. The bandwidth of the system allows the observation of slow oscillations.

- *Scanning along the detector line* in a single shot allows to get a set of plasma parameter profiles. The scanning was realized by variation of the injection angle during the correcting voltage pulse. The scanning time was about 4 ms. The spatial resolution of the measurements is determined by the (5–10) mm sample volume, while the temporal resolution was limited by the data acquisition system (20 kHz).

4.2 Main features of the ECRH H-mode in T-10

Figure 8 shows the time history of a typical shot (central ECRH) with a spontaneous transition to improved confinement, manifesting itself as a spontaneous increase in plasma density accompanied by a decrease in recycling, and an increase in stored energy (enhancement factor attains 1.6) [31].

The main difference with other tokamaks is the long time scale of the L–H transition. During the ECRH phase density, stored energy, recycling and central T_e increase. After L–H transition the plasma density increase is accompanied by an increase in plasma energy and a decrease in recycling, while the electron temperature does no longer increase. In the H-mode an external barrier arises for electrons, whereas the heat transport barrier insignificantly contributes to improved confinement. This phenomenon is similar to those observed during the biased-induced H-mode in TEXTOR-94 and CASTOR. After the L–H transition the increase in density and energy continues up to the end of the ECRH pulse.

The profiles of the plasma density and its gradient (measured with the HIBP) shown in Fig. 9 demonstrate that an external transport barrier arises near the limiter. There is no evidence of a substantial accumulation of impurities in the plasma core in the H-mode. The threshold power for the L–H transition is close to that predicted by the ITER scaling [33].

Typical results of HIBP measurements are presented in Fig. 10 for the case of on-axis ECRH. The quantity $\Delta\varphi$ is defined with respect to the "base" plasma potential φ_B^L in the L-phase of the discharge ($\Delta\varphi = \varphi - \varphi_B^L$). Thus, the data characterize the variations in plasma potential (and, consequently in radial electric field E_r) relative to its value in the L-phase.

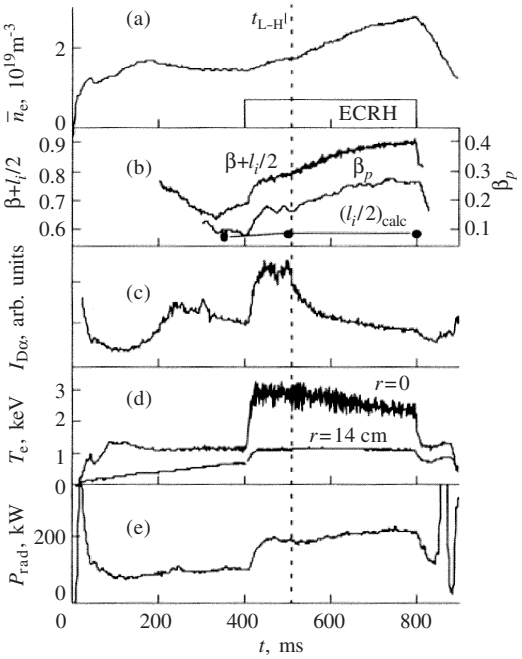

Fig. 8. Time evolution of (a) the mean plasma density; (b) quantities $\beta + l_\mathrm{i}/2$ (data from the plasma equilibrium) and β_p (diamagnetic measurements); (c) intensity of the D_α line; (d) electron temperature; (e) radiated power in the regime with the L-H transition (shot No. 26 154, $B_\mathrm{t} = 2.42$ T, $I_\mathrm{p} = 330$ kA, $q_\mathrm{L} = 2.2$, and $P_\mathrm{ab} = 750$ kW).

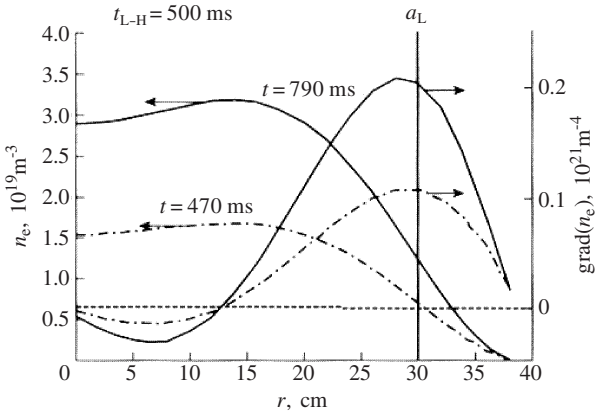

Fig. 9. Profiles of the density and the density gradient in the L-phase ($t = 470$ ms) and at the end of the microwave pulse in the H-phase ($t = 790$ ms).

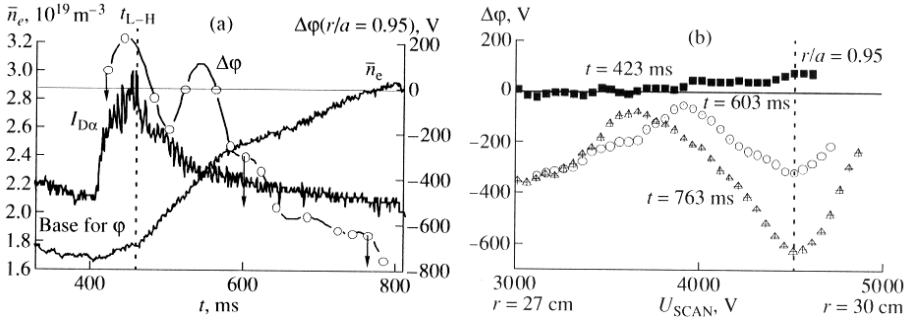

Fig. 10. Results from measurements of the plasma potential $\Delta\varphi$ in the H-mode (B_t = 2.42 T, I_p = 330 kA, q_L = 2.2, and P_{ab} = 750 kW): (a) time evolution of $\Delta\varphi$ for $r(\varphi_{min})$ at $r/a = 0.95$ and (b) radial profiles of $\Delta\varphi$ for the instants indicated by the arrows in the panel (a). The interval for determining the base value of the potential φ_B^L is also shown in the panel (a).

The characteristic features of E_r in H-mode discharges are the following:

1. During the L–H transition, E_r is generated in a narrow region (1.5–2 cm) adjacent to the limiter (a_L = 30 cm).
2. After ECRH switch-on, a positive E_r is generated in this region.
3. During L–H transition, E_r changes strongly. However, its value is low compared to its maximum value at the end of the microwave pulse, when the H-mode is nearly steady state.

Figure 10 shows a plasma profile with a well, meaning that besides the negative E_r, a positive E_r is generated at the inner side of the barrier, the role of which has still to be investigated.

5 Summary

Following the pioneering work on CCT, the research activities on induced radial electric fields in TEXTOR-94 contributed significantly to the understanding of the physics of radial currents, of the H-mode phenomenon and of the effects of E_r on plasma transport and exhaust. The physics of radial current transport was studied on TEXTOR-94 and the radial conductivity in the edge of a tokamak was found to be dominated by recycling (ion-neutral collisions) at the LCFS and by parallel viscosity inside the LCFS. The destruction of parallel viscosity by strong poloidal plasma rotation was verified and found to lead to a bifurcation in the electric field. Global changes of confinement and of plasma profiles and particle transport barriers induced by the presence of positive and negative radial electric fields were determined. H-mode behaviour can be induced both with positive and negative radial electric fields. Radial electric fields were found to strongly affect exhaust, not only in the H-mode. Helium exhaust is particularly difficult in H-mode.

The biasing arrangement and the plasma flow and turbulence measurements on CASTOR offered a first experimental proof that imposing a boundary condition by (non-intrusive) separatrix biasing is an efficient way to create strongly sheared electric fields, thereby affecting plasma flows and de-correlating turbulent structures, and creating an edge transport barrier in the proximity of the separatrix, which leads to improved confinement.

The rotatable Mach probe and the novel "Ideal" Gundestrup probe with its excellent temporal resolution, enabled to measure the parallel and perpendicular plasma flows which are strongly affected in the sheared region, especially in the perpendicular direction. The $\mathbf{E} \times \mathbf{B}$ shear rate for separatrix biasing is larger than for standard biasing schemes, and significantly exceeds the growth rate of unstable turbulent modes. Probe array measurements demonstrated a strong impact on the turbulent structures.

With ECRH alone, a regime with improved confinement is obtained on T-10 with feature resembling those in the H-mode in other tokamaks. The heavy ion beam probe data demonstrated that the time evolution of the plasma potential profile during L–H transition is clearly correlated with that of the edge density profile and the formation of a transport barrier near the limiter.

Similar to the cases of electrode biasing in TEXTOR-94 and CASTOR, the experimentally observed transport barrier in T-10 is a barrier for particles.

The authors are indebted to the TEXTOR-94, CASTOR and T-10 teams. We thank Martin Hron and Jan Horacek (IPP Prague) for providing figures of Section 3.

References

[1] F. Wagner et al.: Phys.Rev.Letters **49** (1982) 1408.

[2] R.J. Taylor et al.: Phys.Rev.Letters **63** (1989) 2365.

[3] R.R. Weynants et al.: Nucl. Fusion **32** (1992) 837.

[4] R.R. Weynants and G.Van Oost.: Plasma Phys. Contr. Fusion **35** (1993) 177.

[5] S. Jachmich et al.: Plasma Phys. Contr. Fusion **40** (1998) 1105.

[6] J. Cornelis et al.: Nucl. Fusion **34** (1994) 171.

[7] H. Van Goubergen et al.: Plasma Phys. Contr. Fusion **41** (1999) L17.

[8] A. Pospieszczyk et al.: J. Nucl. Mat. **162–164** (1989) 574.

[9] D.S. Gray et al.: Nucl. Fusion **38** (1998) 1585.

[10] T.E. Stringer: Nucl. Fusion **32** (1992) 1421.

[11] K.C. Shaing and E.C. Crume, Jr.: Phys. Rev. Lett. **63** (1989) 2369.

[12] A.B. Hassam et al.: Phys. Rev. Lett. **66** (1991) 309.

[13] P.H. Diamond et al.: Phys. Fluids B **3** (1991) 1626.

[14] H-mode Database Working Group: in *1993 Plasma Phys. and Contr. Nucl. Fus. Res.* 1992, IAEA, Vienna, Vol. 3, p. 268.

[15] D. Reiter et al.: Nucl. Fus. **30** (1990) 2141.

[16] D. Hillis et al.: Phys. Rev. Letters **65** (1990) 2382.

[17] R.R. Weynants et al.: Nucl. Fusion **32** (1995) 837.

[18] V. Rozhansky and M. Tendler: *Reviews of Plasma Physics*, Vol. 19 (Ed. B.B. Kadomtsev), New York and London, 1996.

[19] G. Van Oost et al.: Czech. J. Phys. **50**/Suppl. S3 (2000) 11.

[20] J. Stöckel et al.: in *Proc. 27th EPS Conf. Contr. Fusion Plasma Phys.*, Budapest, 2000, p. 1032

[21] M. Tendler: Plasma Phys. Contr. Fusion **39** (1997) B371.

[22] J. Stöckel et al.: Plasma Phys. and Contr. Fusion **41** (1999) A577.

[23] J.P. Gunn: Czech. J. Phys. **48**/Suppl. S3 (1998) 293.

[24] C.S. MacLatchy et al.: Rev. Sci. Instr. **63** (1992) 3923.

[25] K. Dyabilin et al.: in *Proc. of 27th EPS Conf. Contr. Fusion Plasma Phys.*, Budapest, 2000, p. 1653.

[26] J.P. Gunn et al.: Phys. Plasmas **38** (2001) 1995.

[27] S.J. Zweben and R.W. Gould: Nucl. Fusion **25** (1985) 171.

[28] J. Stöckel et al.: J. Tech. Phys. **41**, Special Issue, (2000) 49.

[29] M. Endler et al.: Nucl. Fusion **35** (1995) 1307.

[30] J. Stöckel et al.: in *Proc. 26th EPS Conf. Contr. Fusion Plasma Phys.*, Maastricht, 1999, p. 1589.

[31] V.V. Alikaev et al.: Plasma Phys. Reports **26** (2000) 917.

[32] A. Melnikov et al.: J. Plasma Fusion Res. Series **3** (2000) 46.

[33] Technical Basis for the ITER-FEAT Outline Design, Chap. 1, Sect. 2, p. 3.

[34] J.P. Gunn et al.: Czech. J. Phys. **51** (2001) 1001 (these proceedings).